Letter

# Observation of biexciton emission from single semiconductor nanoplatelets

Lintao Peng,[1] Wooje Cho,[2] Xufeng Zhang,[1] Dmitri Talapin,[1,2] and Xuedan Ma[1,3,4,*]

[1]*Center for Nanoscale Materials, Argonne National Laboratory, Lemont, Illinois 60439, USA*

[2]*Department of Chemistry and James Franck Institute, University of Chicago, Chicago, Illinois 60637, USA*

[3]*Consortium for Advanced Science and Engineering, University of Chicago, Chicago, Illinois 60637, USA*

[4]*Northwestern-Argonne Institute of Science and Engineering, 2205 Tech Drive, Evanston, Illinois 60208, USA*

(Received 14 February 2021; accepted 12 April 2021; published 4 May 2021)

Quasi-two-dimensional semiconductor nanoplatelets (NPLs) are intriguing systems for studying the influence of Auger recombination processes on the multiexciton emission efficiencies in the weak in-plane confinement regime. We investigate CdSe/CdS core/shell NPLs using cryogenic temperature single particle spectroscopy and observe bright biexciton emission at high excitation powers. The average binding energy of the biexcitons is determined to be 16.5 meV. The observed switching between the biexciton and trion states indicates charging-decharging dynamics of the NPLs mediated by the Auger ionization process. These findings are highly relevant for harvesting efficient biexciton emission for energy, lighting, and quantum applications.

DOI: 10.1103/PhysRevMaterials.5.L051601

Quantum confinement in low-dimensional semiconductor materials is often manifested as reduced dielectric screening and strong many-body Coulomb interaction [1,2], which can lead to the formation of stable excitons and higher-order excitonic states with large binding energies and oscillator strengths. Of particular interest are biexcitons, bound states of two electron-hole pairs, due to their applications in low-threshold lasing, energy harvesting, and quantum cascade emission of photon pairs [3–6]. While biexciton emission in highly confined quantum dots is typically diminished due to ultrafast nonradiative Auger recombination processes, control over electron and hole wave function overlaps has been demonstrated to be an effective strategy for suppressing Auger processes and enhancing multiexciton emission [7,8].

Semiconductor nanoplatelets (NPLs) are quasi-two-dimensional nanostructures that are tens of nanometers in lateral dimensions but only a few atomic layer thick. Due to the strong quantum confinement in the thickness direction, NPLs can present narrower optical spectra compared to their quantum dot counterparts [9]. The spreading of the exciton wave functions over the extended lateral dimensions [10,11] has led to the observation of giant oscillator strength and fast radiative decay rates in NPLs [12,13]. Moreover, they can serve as model systems for tuning the Auger recombination rates and biexciton states due to their adjustable plate geometries. Specifically, an increase in the NPL lateral dimension can result in a reduction in the Auger recombination rate and consequently more efficient multiexciton emission [12,14], attested by previous observation of bright trion emission from the NPLs [10,15]. However, despite the importance of biexciton emission in energy and quantum related applications, study of biexciton states in nanoplatelets has remained sparse [3,16].

Here, we investigate CdSe/CdS core/shell NPLs using cryogenic temperature single particle optical spectroscopy. An advantage of performing measurements on single NPLs is that it could help reveal the intimate details of the nanoscale photophysics such as homogeneous broadening and local electrostatic field fluctuations of individual NPLs. We demonstrate evidence of biexciton emission in the NPLs which exhibits characteristic spectral correlation with single exciton emission and superlinear power dependency. Biexciton binding energies of 10–28 meV with an average value of 16.5 meV were discovered. Switches between trion and biexciton emission were also observed, which allows for the derivation of the relative energy levels in the studied NPLs. These findings provide evidence for the suppressed Auger recombination processes and efficient multiexciton emission in NPLs.

The NPLs used in this study were synthesized following a previously published colloidal atomic layer deposition technique [17]. Each NPL was comprised of four monolayer-thick (∼1.2 nm) CdSe cores conformally coated with four monolayers of CdS shells. The average lateral dimension of the NPLs was determined to be around $21 \times 7$ nm$^2$ using transmission electron microscopy [Fig. 1(a)]. These lateral dimensions are well above the exciton Bohr radius of CdSe (5.6 nm) [18], thus placing the NPLs in the weak and medium confinement regimes in the length and width directions, respectively. Figure 1(b) shows the absorption and emission spectra of the NPL solutions at room temperature. Two characteristic features can be resolved in the absorption spectra, which can be assigned to the electron-heavy hole (HH, lower energy) and electron-light hole (LH, higher energy) transitions [9]. The emission occurs at a small Stokes shift (22 meV) from the electron-heavy hole absorption peak.

NPL samples for cryogenetic temperature optical measurements were prepared by diluting the stock solutions followed by spin coating them onto precleaned quartz substrates. The prepared samples were then loaded into a continuous-flow

*xuedan.ma@anl.gov

 

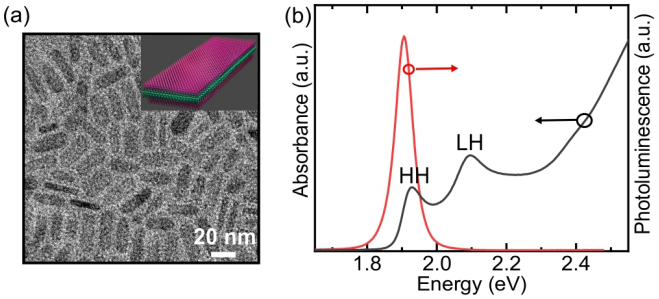


FIG. 1. (a) Transmission electron microscope image of the NPLs. Inset: a sketch of the NPLs. (b) Absorption (black) and emission (red) spectra of the NPL solutions at room temperature. HH: heavy hole; LH: light hole.

liquid helium cryostat that is installed on a home-built microphotoluminescence setup. We use a 400 nm diode laser to excite the NPLs into the continuum band by focusing the laser beams onto the samples using a microscope objective (NA = 0.7, 40×). The pulse width and repetition rate of the laser are around 50 ps and 5 MHz, respectively. Photoluminescence (PL) from the NPLs was collected by the same objective and sent to a charge-coupled device equipped on a 500 mm spectrometer for imaging and spectroscopic measurements, or to two single-photon avalanche diodes in a Hanbury Brown-Twiss configuration for time-resolved and time-correlated single photon counting experiments. Unless otherwise stated, all the optical measurements were performed at 5 K.

In order to ensure that single NPLs instead of their clusters were measured each time, we start by performing second-order photon correlation [$g^{(2)}(\tau)$] studies of the NPLs. In this mode, the laser excitation power was kept sufficiently low so that the average absorbed photons per pulse was below 0.5. Figure 2(a) shows a representative $g^{(2)}(\tau)$ trace of a NPL. By defining the area ratio between the center peak and the side peaks of the $g^{(2)}(\tau)$ trace as $R$, we obtain its value to be 0.96. For a typical quantum dot, the so-called photon antibunching manifested as $R \to 0$ in the $g^{(2)}(\tau)$ trace is expected, which indicates that the probability of detecting two or more photons per excitation pulse is low. The observation of the nonzero $R$ value could have two origins: the excitation of more than one NPL in the laser beam spot or quantum cascade emission of biexcitons [12,19]. To identify the origin, we apply a time gating technique [20,21] to the $g^{(2)}(\tau)$ measurements. Based on the fact that biexcitons decay faster than single excitons [22] and by constructing the $g^{(2)}(\tau)$ traces only using photons with decay times much longer than the biexciton lifetime, we are able to exclude the contributions of the biexciton emission in the $R$ values and only single photon emission is considered. Figure 2(b) shows the $g^{(2)}(\tau)$ trace after applying a gate time of 5 ns. Apparently the $R$ value has decreased to nearly zero. This observation reveals that the nonzero $R$ value observed in Fig. 2(a) is indeed caused by biexciton emission instead of the excitation of multiple NPLs. By applying this approach, we are able to distinguish single NPLs from multiple ones even though both could give rise to nonzero $R$ values. We only consider those NPLs exhibiting gated $R$ value of zero to be single and further investigate them.

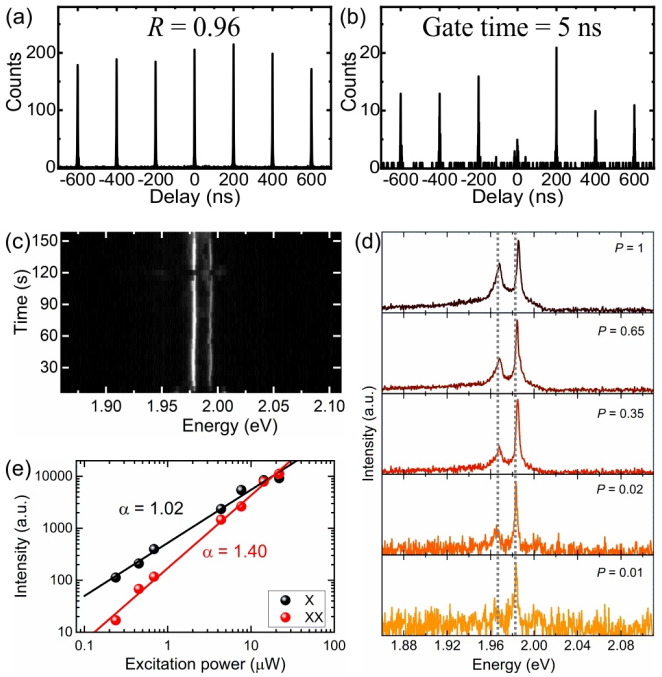


FIG. 2. (a) A second-order photon correlation [$g^{(2)}(\tau)$] trace of a NPL. (b) The $g^{(2)}(\tau)$ trace after applying a gate time of 5 ns. (c) Time-dependent PL spectra of an individual NPL. The integration time of each frame is 5 s. (d) PL spectra of a NPL at various excitation powers. The excitation power is shown to be normalized to the maximum power. (e) Pump-power dependent PL integral of the two emission peaks in (d). The lines are power-law fits to the data.

Emission spectra of the single NPLs at cryogenic temperatures can help reveal their electronic fine structures and related photophysics. Figure 2(c) shows a time sequence of photoluminescence spectra from a NPL. Two distinct PL peaks can be observed with an almost constant energy spacing of around 15.4 meV between them. Fluctuations in local electrostatic fields can induce changes in the exciton binding energies, leading to spectral shift or broadening, as observed for both PL peaks in Fig. 2(c) [23]. This kind of spectral diffusion behavior has also been observed in other quantum confined systems and is typically attributed to fluctuations in surface charges [24]. Moreover, the two PL peaks demonstrate correlated on/off blinking behavior, as evident at around 0 s and 120 s in Fig. 2(c). The correlated PL peaks outline a possible emission cascade initialized by a biexciton state [25].

We further perform excitation power-dependent studies of such correlated PL features [Fig. 2(d)]. At low excitation powers, the high-energy peak dominates, but as we increase the power, the low-energy peak becomes more prominent. A careful inspection of the power-dependent PL integral intensity reveals distinctively different behaviors of the two peaks, with the intensity of the low-energy peak increasing much rapidly compared to the high-energy peak [Fig. 2(e)]. Fitting of the power-dependent PL intensity data with power law functions $I \propto P^{\alpha}$ yields a linear coefficient $\alpha = 1.02$ for the high-energy peak and a superlinear coefficient $\alpha = 1.40$ for the low-energy peak. This superlinear dependency together with the correlation between the two PL features allows us to

assign the high- and low-energy peaks to single excitons and biexcitons, respectively [26,27]. For a quantum emitter in full thermal equilibrium, the biexciton density is expected to grow quadratically with respect to the single exciton density (i.e., $\alpha = 2$), but instead $\alpha = 1.2$–$1.9$ has often been observed [26] and it is typically attributed to the lack of thermal equilibrium between the involved states [28]. We believe the $\alpha = 1.40$ coefficient observed here is due to a similar mechanism caused by the short lifetimes of the single excitons [9,10] and the weak exciton-phonon interactions in CdSe NPLs at low temperatures [29].

We observe biexciton emission in around 32% of the studied NPLs (22 out of 68). From the spectral positions of the exciton and biexciton emission, we can derive the biexciton binding energy $E^b_{xx}$. Specifically, biexciton binding energy is defined as $E^b_{xx} = 2E_x - E_{xx}$, where $E_x$ and $E_{xx}$ are the energies of the single exciton and biexciton states, respectively [Fig. 3(a)]. Since the radiative decay of a biexciton results in a single exciton, $E_{xx} = \hbar\omega_{xx} + E_x$, where $\hbar\omega_{xx}$ is the biexciton emission energy. Given that $E_x = \hbar\omega_x$ with $\hbar\omega_x$ being the exciton emission energy, the biexciton binding energy equals to the energy shift between the single exciton and biexciton emission: $E^b_{xx} = \hbar\omega_x - \hbar\omega_{xx}$. For the NPLs studied here, $E^b_{xx}$ varies in the range of 10–28 meV with an average value of 16.5 meV [Fig. 3(b)]. This variation in the binding energy could be related to the small deviations in the NPL sizes as well as influences from local environmental perturbations. The average biexciton binding energy value obtained here is smaller than those reported for epitaxially grown quantum dots [30] but larger than those of quantum wells [31], which is consistent with the quasi-two-dimensional nature of the NPLs. As the exciton localization degree increases, which is manifested as an increase in the exciton emission energy, the biexciton binding energy would increase accordingly [32]. No systematic dependency between the biexciton binding energy and exciton emission energy is observed here [Fig. 3(c)]. This may be due to the narrow emission energy window of the NPLs and the spectral diffusion which make the observation of any confinement-induced enhancement in the biexciton binding energy negligible [30].

For the NPLs that exhibit biexciton emission, we sometimes observe abrupt switching from the two correlated exciton-biexciton emission peaks to a third feature, as exemplified in Figs. 3(d) and 3(e): When the biexciton-exciton cascade emission turns dark, the third feature turns bright, and vice versa. The energy separation between this third feature and the exciton emission is around 8.2 meV. This energy separation and the correlated switching characteristics of the third feature with single exciton emission lead us to its assignment as the trion emission, as was previously discovered in such NPLs [10]. When the NPL undergoes photoexcitation upon illumination, it creates single excitons at low excitation powers but generates biexcitons at high powers, which can lead to the biexciton and single exciton emission [I in Fig. 3(f)]. However, it has been reported [10,15] that at low temperatures, the NPLs tend to turn into charged states either through trapping of surface charges [II in Fig. 3(f)] or Auger ionization processes [III in Fig. 3(f)]. The excited state of a charged NPL, i.e., the trion state, can lead to the trion emission [IV in Fig. 3(f)]. The trapping and detrapping of the extra charge

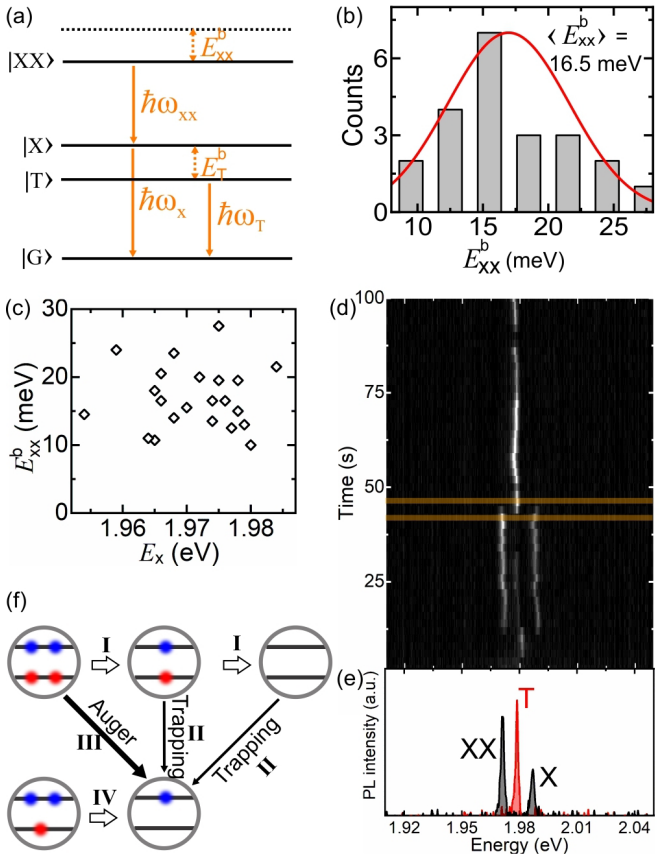


FIG. 3. (a) Energy levels in the studied NPLs. |G⟩, |T⟩, |X⟩, and |XX⟩ represent the ground, trion, exciton, and biexciton states, respectively. $E^b_T$ and $E^b_{xx}$ are the binding energies of the trions and biexcitons. (b) Histogram of the biexciton binding energies. (c) The biexciton binding energies plotted as a function of the corresponding exciton emission energy. (d) A representative time sequence of PL spectra of a NPL showing switching between the biexciton and trion states. The integration time of each spectrum is 2 s. (e) PL spectra corresponding to the highlighted time regimes in (d). X, XX, and T represent excitons, biexcitons, and trions, respectively. (f) Sketch of the transitions among biexciton, trion, and exciton states. The example is given for a negatively charged NPL. I: cascade emission of a biexciton to a single exciton. II: trapping of surface charges leading to charged NPLs. III: Auger ionization resulting in charged NPLs. IV: trion emission.

results in the observation of switches between the biexciton-exciton emission and trion emission. We note though that the charging-decharging process can happen very fast and take place within the experimental integration time, which explains the observation of both types of spectral features at around 15–35 s in Fig. 3(d). For the NPLs exhibiting biexciton emission, the transition typically happens between the biexciton-exciton and trion states (III and IV) but rarely between the single exciton and trion states (II and IV), which indicates that in these NPLs, the charged states are predominantly formed through Auger processes. Moreover, the binding energies of the biexcitons and trions allow us to derive the relative energy levels of these states for the NPLs studied here [Fig. 3(a)].

In conclusion, we investigate CdSe/CdS core/shell NPLs using cryogenic temperature single particle spectroscopy and observe bright biexciton emission at high excitation powers. This provides evidence for the suppressed Auger recombination processes in these quasi-two-dimensional NPLs and the potential to harvest bright multiexciton emission from them. The binding energy of the biexcitons is determined to be around 16.5 meV. The direct transition between the biexciton and trion states indicates that the biexciton states in the NPLs are still prone to Auger processes. The findings obtained in this study may have important implications for the development of lightening devices and photovoltaics based on the NPLs [33–35].

This work was performed, in part, at the Center for Nanoscale Materials, a U.S. Department of Energy Office of Science User Facility, and supported by the U.S. Department of Energy, Office of Science, under Contract No. DE-AC02-06CH11357. X.M. acknowledges support from the Center for Molecular Quantum Transduction (CMQT), an Energy Frontier Research Center funded by the U.S. Department of Energy (DOE) under Grant No. DE-SC0021314. The work on nanoplatelet synthesis was supported by the National Science Foundation under Award No. DMR-1905290 and by the Department of Defense (DOD) Air Force Office of Scientific Research under Grant No. FA9550-15-1-0099.

[1] X. Cartoixà and L.-W. Wang, Phys. Rev. Lett. **94**, 236804 (2005).
[2] A. Franceschetti and A. Zunger, Phys. Rev. Lett. **78**, 915 (1997).
[3] J. Q. Grim, S. Christodoulou, F. D. Stasio, R. Krahne, R. Cingolani, L. Manna, and I. Moreels, Nat. Nanotechnol. **9**, 891 (2014).
[4] K. J. Karki, J. R. Widom, J. Seibt, I. Moody, M. C. Lonergan, T. Pullerits, and A. H. Marcus, Nat. Commun. **5**, 5869 (2014).
[5] R. M. Stevenson, R. J. Young, P. Atkinson, K. Cooper, D. A. Ritchie, and A. J. Shields, Nature (London) **439**, 179 (2006).
[6] L. Peng, X. Ma, H. Zhu, O. Chen, and W. Wang, Phys. Rev. B **102**, 035437 (2020).
[7] W. K. Bae, L. A. Padilha, Y.-S. Park, H. McDaniel, I. Robel, J. M. Pietryga, and V. I. Klimov, ACS Nano **7**, 3411 (2013).
[8] M. Zavelani-Rossi, M. G. Lupo, F. Tassone, L. Manna, and G. Lanzani, Nano Lett. **10**, 3142 (2010).
[9] S. Ithurria, M. D. Tessier, B. Mahler, R. P. S. M. Lobo, B. Dubertret, and A. L. Efros, Nat. Mater. **10**, 936 (2011).
[10] L. Peng, M. Otten, A. Hazarika, I. Coropceanu, M. Cygorek, G. P. Wiederrecht, P. Hawrylak, D. V. Talapin, and X. Ma, Phys. Rev. Materials **4**, 056006 (2020).
[11] N. F. Hartmann, M. Otten, I. Fedin, D. Talapin, M. Cygorek, P. Hawrylak, M. Korkusinski, S. Gray, A. Hartschuh, and X. Ma, Nat. Commun. **10**, 3253 (2019).
[12] X. Ma, B. T. Diroll, W. Cho, I. Fedin, R. D. Schaller, D. V. Talapin, S. K. Gray, G. P. Wiederrecht, and D. J. Gosztola, ACS Nano **11**, 9119 (2017).
[13] A. Naeem, F. Masia, S. Christodoulou, I. Moreels, P. Borri, and W. Langbein, Phys. Rev. B **91**, 121302(R) (2015).
[14] Q. Li and T. Lian, Nano Lett. **17**, 3152 (2017).
[15] F. V. Antolinez, F. T. Rabouw, A. A. Rossinelli, R. C. Keitel, A. Cocina, M. A. Becker, and D. J. Norris, Nano Lett. **20**, 5814 (2020).
[16] F. G. Flórez, L. D. A. Siebbeles, and H. T. C. Stoof, Phys. Rev. B **102**, 115302 (2020).
[17] S. Ithurria and D. V. Talapin, J. Am. Chem. Soc. **134**, 18585 (2012).
[18] A. I. Ekimov, F. Hache, M. C. Schanne-Klein, D. Ricard, C. Flytzanis, I. A. Kudryavtsev, T. V. Yazeva, A. V. Rodina, and A. L. Efros, J. Opt. Soc. Am. B **10**, 100 (1993).
[19] J. Zhao, O. Chen, D. B. Strasfeld, and M. G. Bawendi, Nano Lett. **12**, 4477 (2012).
[20] B. D. Mangum, Y. Ghosh, J. A. Hollingsworth, and H. Htoon, Opt. Express **21**, 7419 (2013).
[21] H. Abudayyeh, B. Lubotzky, S. Majumder, J. A. Hollingsworth, and R. Rapaport, ACS Photon. **6**, 446 (2019).
[22] Y.-S. Park, W. K. Bae, J. M. Pietryga, and V. I. Klimov, ACS Nano **8**, 7288 (2014).
[23] X. Ma, O. Roslyak, F. Wang, J. G. Duque, A. Piryatinski, S. K. Doorn, and H. Htoon, ACS Nano **8**, 10613 (2014).
[24] S. A. Empedocles and M. G. Bawendi, Science **278**, 2114 (1997).
[25] P. Tamarat, L. Hou, J.-B. Trebbia, A. Swarnkar, L. Biadala, Y. Louyer, M. I. Bodnarchuk, M. V. Kovalenko, J. Even, and B. Lounis, Nat. Commun. **11**, 6001 (2020).
[26] Y. You, X.-X. Zhang, T. C. Berkelbach, M. S. Hybertsen, D. R. Reichman, and T. F. Heinz, Nat. Phys. **11**, 477 (2015).
[27] H. Htoon, A. V. Malko, D. Bussian, J. Vela, Y. Chen, J. A. Hollingsworth, and V. I. Klimov, Nano Lett. **10**, 2401 (2010).
[28] R. T. Phillips, D. J. Lovering, G. J. Denton, and G. W. Smith, Phys. Rev. B **45**, 4308 (1992).
[29] A. W. Achtstein, A. Schliwa, A. Prudnikau, M. Hardzei, M. V. Artemyev, C. Thomsen, and U. Woggon, Nano Lett. **12**, 3151 (2012).
[30] B. Patton, W. Langbein, and U. Woggon, Phys. Rev. B **68**, 125316 (2003).
[31] J. Singh, D. Birkedal, V. G. Lyssenko, and J. M. Hvam, Phys. Rev. B **53**, 15909 (1996).
[32] G. Hönig, G. Callsen, A. Schliwa, S. Kalinowski, C. Kindel, S. Kako, Y. Arakawa, D. Bimberg, and A. Hoffmann, Nat. Commun. **5**, 5721 (2014).
[33] C. She, I. Fedin, D. S. Dolzhnikov, P. D. Dahlberg, G. S. Engel, R. D. Schaller, and D. V. Talapin, ACS Nano **9**, 9475 (2015).
[34] X. Ma, B. T. Diroll, W. Cho, I. Fedin, R. D. Schaller, D. V. Talapin, and G. P. Wiederrecht, Nano Lett. **18**, 4647 (2018).
[35] S. Luo, M. Kazes, H. Lin, and D. Oron, J. Phys. Chem. C **121**, 11136 (2017).